PROFESSIONAL PAPER SJ2006-PP3

DISTRIBUTION OF SUBMERGED AQUATIC VEGETATION IN THE LOWER ST. JOHNS RIVER: 2004 ATLAS

Professional Paper SJ2006-PP3

DISTRIBUTION OF SUBMERGED AQUATIC VEGETATION IN THE LOWER ST. JOHNS RIVER: 2004 ATLAS

by

Dean R. Dobberfuhl, Ph.D., and Courtney Hart

St. Johns River Water Management District
Palatka, Florida

2006

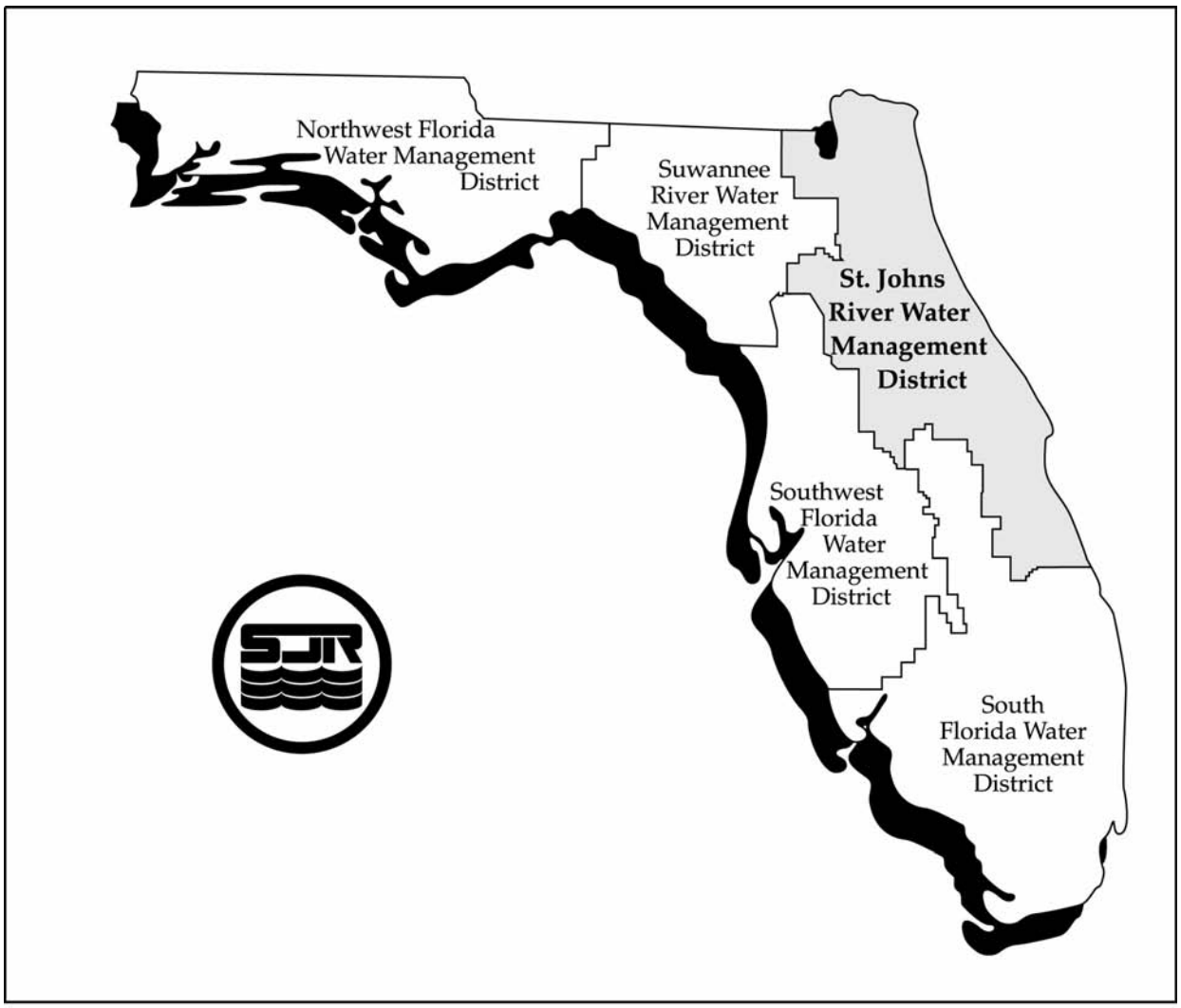

The St. Johns River Water Management District (SJRWMD) was created by the Florida Legislature in 1972 to be one of five water management districts in Florida. It includes all or part of 18 counties in northeast Florida. The mission of SJRWMD is to ensure the sustainable use and protection of water resources for the benefit of the people of the District and the state of Florida. SJRWMD accomplishes its mission through regulation; applied research; assistance to federal, state, and local governments; operation and maintenance of water control works; and land acquisition and management.

This document is published to disseminate information collected by SJRWMD in pursuit of its mission. Copies of this document can be obtained from:

Library
St. Johns River Water Management District
4049 Reid Street • P.O. Box 1429
Palatka, FL 32178-1429

Phone: (386) 329-4132

Professional Paper SJ2006-PP3

DISTRIBUTION OF SUBMERGED AQUATIC VEGETATION IN THE LOWER ST. JOHNS RIVER: 2004 ATLAS

Dean R. Dobberfuhl, Ph.D., and Courtney Hart

ABSTRACT

This atlas contains Lower St. Johns River Basin submerged aquatic vegetation (SAV) data for the years 2003 and 2004. Ground-truthing transects were performed and mapped for each year. Hyperspectral imagery was obtained and mapped for only 2003. Hyperspectral imagery classification was generally successful and appeared to identify a greater proportion of the existing SAV than previous attempts using true-color photo interpretation. Based on the imagery classification, 2,140 acres of SAV were mapped within the mainstem of the lower basin. In some cases, imagery classification and transect data gave divergent bed-size estimates. Reasons for those discrepancies are briefly discussed.

INTRODUCTION

Submerged aquatic vegetation (SAV) plays an important role in many aquatic ecosystems, particularly in shallow lakes (Scheffer 1998). It is important for anchoring sediment, sequestering nutrients, serving as a food resource and as nursery habitat (Dennison et al., 1993). SAV is an important food source and habitat for a number of organisms in the Lower St. Johns River Basin (LSJRB). Manatees graze the deepwater edge of the SAV beds and use the shallow areas for cover (reviewed in Burns et al. 1997). Fish rely on SAV beds for predator evasion and increased foraging opportunities (Rozas and Odum 1988, Heck and Crowder 1991, Jordan et al. 1996), as do insects (Batzer and Wissinger 1996, Lombardo 1997, Solimini et al. 1997). SAV beds in the LSJRB have three-fold-higher fish abundance and 15-fold-higher invertebrate abundance than do adjacent sand flats (D. Dobberfuhl, unpublished data). Thus SAV-based production rates are disproportionately higher than other areas of the river and are critically important to the overall health of the system.

The current SAV mapping effort began, in 1995, to evaluate the quality and distribution of estuarine and freshwater submerged habitats. This ongoing effort is designed to quantify ecosystem change in response to restoration efforts and to provide information necessary for the development of pollutant load reduction goals and total maximum daily loads.

True-color aerial imagery was obtained in 1998 and 2001. Photo interpretation and delineation of the grass beds in the 1998 imagery underestimated grass bed extent at

approximately 50% of the ground-truthing transects (Dobberfuhl 2002). Photo interpretation and delineation of the 2001 imagery was performed on computer monitors by using scanned aerial imagery. This methodology was unsuccessful and failed to identify SAV in many areas of the river (Dobberfuhl and Trahan 2003). In 2003 the decision was made to obtain hyperspectral imagery, focusing on those spectral bands thought to be characteristic of important vegetative and benthic features. This imagery appears to be more sensitive than the true-color imagery previously obtained and better characterizes grass bed features.

This edition of the SAV atlas includes data for the year 2003 and 2004. Two independent measures of SAV spatial extent were performed in 2003 and compared to provide an accuracy estimate for hyperspectral imagery classification. These data and maps are presented as a continuing series of atlases documenting distribution and change of SAV in the LSJRB.

METHODS

Ground-Truth Transects

Seventy-five sites were selected to ground-truth the aerial surveys. At each site, one transect was run from the shoreline to beyond the terminus of the SAV bed. The line-intercept method was used to record species present and percent cover; transect length was recorded, and the two endpoints for each transect were recorded by using geographic information system (GPS). Transect length and the georeference of endpoints were entered into GIS. Transect length was compared to spatial coverages derived from hyperspectral image classification to assess the relative accuracy of the classified images.

Hyperspectral Image Analysis

Imagery—The LSJRB received 67 hyperspectral swaths that covered the lower St. Johns River shoreline in addition to the shoreline of Crescent Lake (Figure 1). The imagery was collected September 13–18, 2003 (HDI, Halifax, Nova Scotia, Canada), using a compact airborne spectrographic imager (CASI) sensor (ITRES, Calgary, Alberta, Canada). The resulting images have 2-meter (m) pixels and a swath width of 512 pixels, or 1024 m, and swath length of 10 to 12 kilometers (km) (Figure 2). Data collection was timed to prevent shadows from riverside trees from interfering with the sensor's view of the water and SAV near shore. Five of the 67 images were used to develop the classification methodology.

Several processes were run on the images before delivery by the vendor, including radiometric correction, across-track illumination correction, geocorrection, and correction to DOQs. Radiometric correction procedures compensate

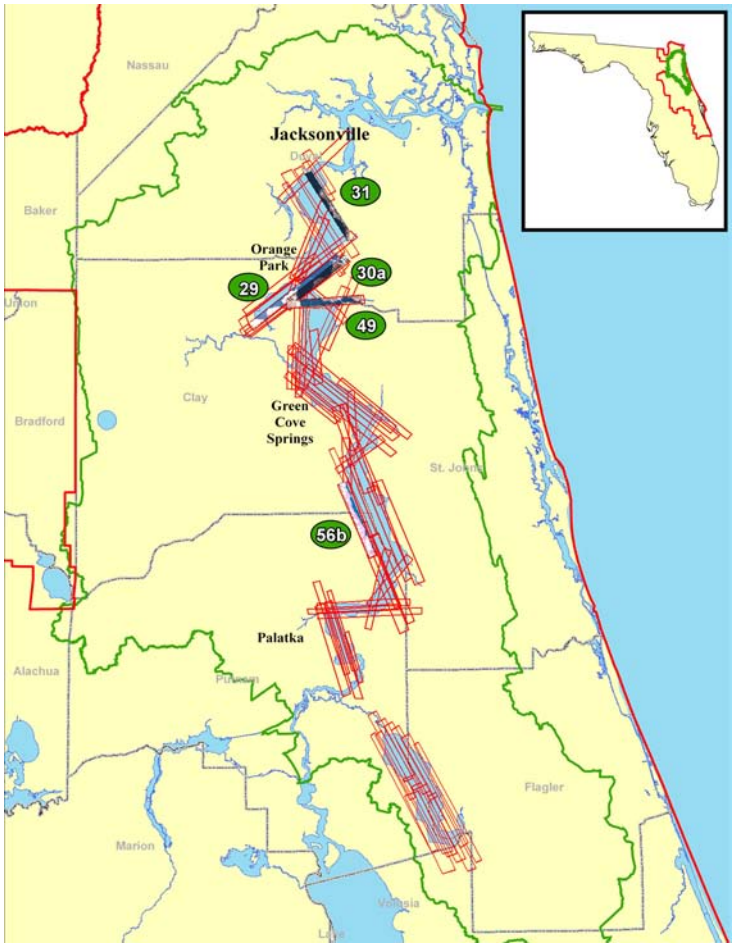

Figure 1. Location of 67 raw images and five pilot study images

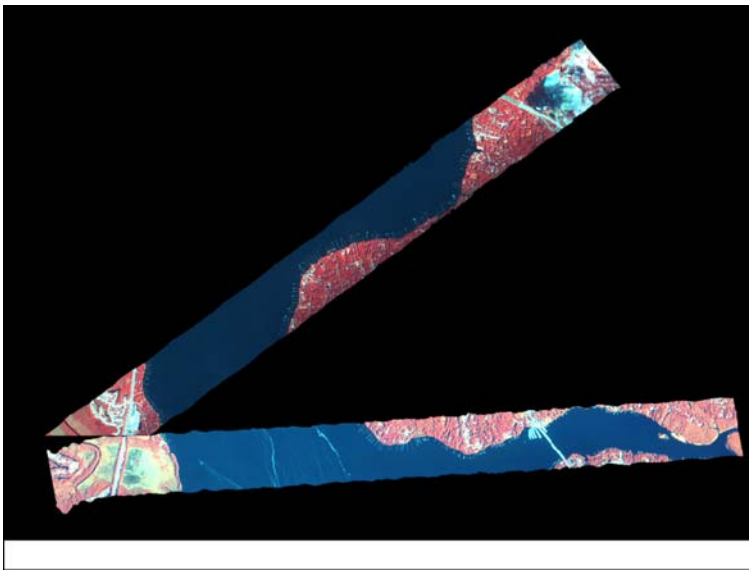

Figure 2. Images 30a (top) and 49

for variations in optical transmission and sensor sensitivity. This process also removes remnants from electronic offset, frame shift smear, and scattered light and calibrates the pixel digital numbers (DN) to Spectral radiance units (SRU), with SRU equal to one micro-watt per square centimeter steradian nanometer, which also can be written

$$SRU = 1\ \mu W cm^{-2} sr^{-1} nm^{-1}.$$

Across-track illumination correction is performed to minimize the distortion and increase in DN values that may occur near the edges of a flightline. The images were geocorrected by using data collected from onboard GPS and gyroscopic equipment to calculate ground position. The images were also geocorrected to 2004 (ADS-40 airborne imagery) set of 1 m digital orthophoto quarter-quadrangles (DOQQs) to produce a product with tighter geodetic control. The DOQQS are in UTM (zone 17), NAD83 (HARN) coordinates, which according to St. Johns River Water Management District (SJRWMD 2005), agrees with the 2–4 m of the 1999 U.S. Geological Survey (USGS) DOQQ set, which has a positional accuracy standard of ± 10 m for 90% of well-defined features (USGS 2004).

Spectral Bands and Bandwidths—Hyperspectral data was collected in 19 different bands of varying widths across the visible (400 [nanometer] nm to 700 nm) and near infrared (700 nm to 1300 nm) range of the electromagnetic spectrum (Table 1). Each band collects information in a different portion of the electromagnetic spectrum and, therefore, may be able to contribute to identifying unique features on the earth's surface. Most objects reflect energy in unique patterns across the electromagnetic spectrum, and bands and bandwidths should be selected to allow that variation to appear without creating unmanageable amounts of data. Water absorbs most wavelengths in the near infrared, so the majority of the most useful information regarding SAV will come from the visible range.

Table 1. Band ranges and bandwidths

Band	Range	Bandwidth (nm)
1	442.1 ± 10.3 nm	20.6
2	464.3 ± 10.4 nm	20.8
3	487.7 ± 13.2 nm	26.4
4	508.0 ± 7.6 nm	15.2
5	524.9 ± 7.6 nm	15.2
6	541.7 ± 7.7 nm	15.4
7	554.8 ± 5.8 nm	11.6
8	565.2 ± 4.9 nm	9.8
9	574.6 ± 4.9 nm	9.8
10	584.9 ± 5.8 nm	11.6
11	595.3 ± 4.9 nm	9.8
12	604.7 ± 4.9 nm	9.8
13	615.1 ± 5.8 nm	11.6
14	627.4 ± 4.9 nm	9.8
15	654.9 ± 5.8 nm	11.6
16	684.3 ± 4.9 nm	9.8
17	696.7 ± 7.8 nm	15.6
18	715.8 ± 9.7 nm	19.4
19	845.0 ± 20.3 nm	40.6

nm = nanometers

Image Processing—ERDAS Imagine (Leica Geosystems, Norcross, Ga.) and ENVI (Research

Systems Inc., Boulder, Colo.) were used for image processing. Imagine has the ability to handle and process very large image files while ENVI has strengths in dealing with hyperspectral imagery. ArcView and ArcGIS (Environmental Systems Research Institute, Redlands, Calif.) were used for GIS work.

Before creating a classification scheme, each individual image swath was equalization-stretched and calibrated to create uniformity throughout the images. A radiance equalization-stretch was developed to correct for lingering swath-to-swath variation, and a reflectance calibration methodology was developed to calibrate remotely sensed spectra to ground-collected spectra. This process permits comparisons between images and allows spectral signatures collected from one image to be applied to other images.

Equalization-Stretch—Images were given a radiance equalization-stretch to reduce between-swath variations resulting from illumination differences. Image 29-2 was selected to be the primary swath since it would also serve as the basis of the following calibration efforts. The range of secondary swaths (images 30a, 31, 49, and 56b) were compared to the primary swath, and a linear function was developed for each band of the secondary swath, such as

$$SR_{n,i} = A_{n,i} * DN_i + B_{n,I}$$

where $SR_{n,i}$ is the stretched radiance in band *i*, DN_i is the digital number for band *i*, and $A_{n,i}$ and $B_{n,i}$ are the slope and intercept coefficients for band *i*. In essence, the secondary swath is squeezed or stretched (via slope) to match the range of the parent swath and is then shifted higher or lower from its origin to that of the primary swath (via intercept).

Calibration—After equalization-stretch, images were calibrated based on the known reflectance of two targets found in image 29-2: a bright target (white sand parking lot) and a dark target (deep open-river water). Reflectance measurements of these two targets had been collected at the time of the 2003 airborne data collection using a spectro-radiometer at previously identified sites. These measurements were then convolved to match the spectral ranges of the 19 bands of the imagery. The bright-target DN statistical extract was obtained from the region of interest (ROI) on the image, while the DN statistical extract of dark river water was obtained from a representative dark-target ROI. A linear calibration equation was then developed for each band, such as

$$SR_i = A_i * DN_i + B_i$$

where SR_i is the spectral reflectance in band *i*, DN_i is the digital number for band *i*, and A_i and B_i are the slope and intercept coefficients for band *i*. The calibration was applied to all of the images, including the

unstretched primary swath, image 29-2.

Classification—Classifying an image involves giving each pixel in the image a class designation based on its value across all bands. There are two major types of classification schemes: unsupervised and supervised. Unsupervised classifications allow the computer processing the data to identify classes based purely on the digital number (DN) of each pixel in each band. Each individual pixel is compared to other pixels, and they are then divided into clusters based on the similarities of their DN combination values. The objective is to group spectral response patterns into clusters that are statistically separable. Supervised classifications are generally more accurate because they include analyst-specified spectral information developed from specified locations in the image. Training sites are identified by the user, and the spectral signatures from those areas guide the model as it classifies the remaining pixels in the image into the designated class types.

For this project, we selected a type of supervised classification scheme uniquely developed for use with hyperspectral data—the spectral angle mapper (SAM) classification scheme. SAM is a physically based spectral classification scheme that uses an n-dimensional angle to match pixels to reference spectra. The algorithm used in the SAM scheme determines the similarity between two spectra by determining the "spectral angle" between them. It uses the direction of the spectra and not its length or magnitude; therefore, all illumination possibilities are treated equally. When used with calibrated data, this method is relatively insensitive to illumination and albedo effects. With SAM, smaller angles represent closer matches of pixels to reference spectra, however, any pixels that do not fall into the angle range of any of the classes will remain unclassed.

Training Data—Training data for the SAM classification scheme were created with the use of transect data that had been collected along the river in 2003. The lower basin of the St. Johns River has 20 permanent monitoring sites where GPS-based transect data are collected annually. Each of the four secondary swaths covers one of the permanent monitoring sites, and each site has five transects within a 50-meter length of the shoreline, where detailed data is collected concerning the species, plant density, and canopy height of the vegetation the entire length of the bed (Figure 3). With this information, regions of interest (ROIs) were digitized on-screen so that polygons in the hyperspectral image could be captured to show medium-to-high density SAV beds. Likewise, additional ROIs were digitized to capture the spectral signatures of other class types, including urban areas, tree cover, and water in each

of the four secondary swaths (Figure 4).

Spectral Signatures—Using the digitized ROIs, the spectral signatures of all 19 bands for the four class types can be compared. Urban areas and areas with tree cover are spectrally distinct and are easily distinguished. However, it is more important, and more difficult, to find spectral separability between water and SAV. Across all four secondary images, bands 1 through 17 show little or no difference in the reflectance values of water and SAV. However, band 18 shows a distinctive dip for water and a

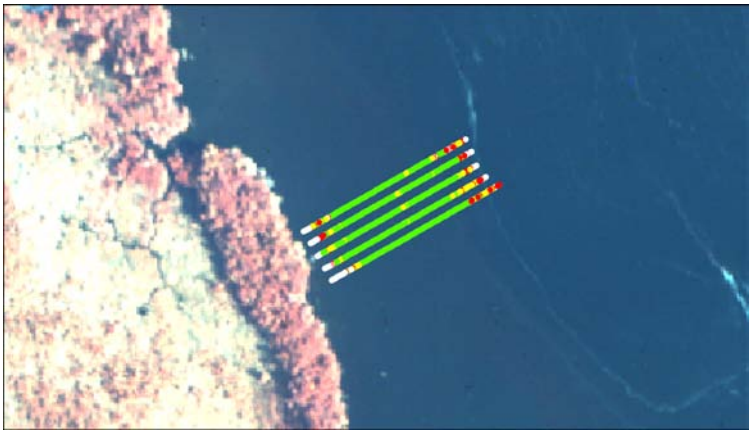

Figure 3. Transects used for classification from image 49

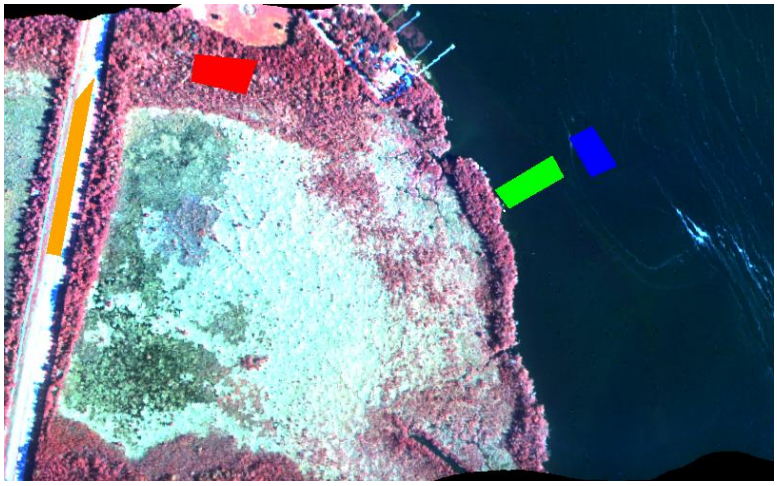

Figure 4. Regions of interest for four classes in image 49

significant peak for SAV (Figures 5a and 5b). Of the 19 bands available in this data set, the spectral separation of water and SAV is dependent on this single band and allows for the differentiation of water and SAV.

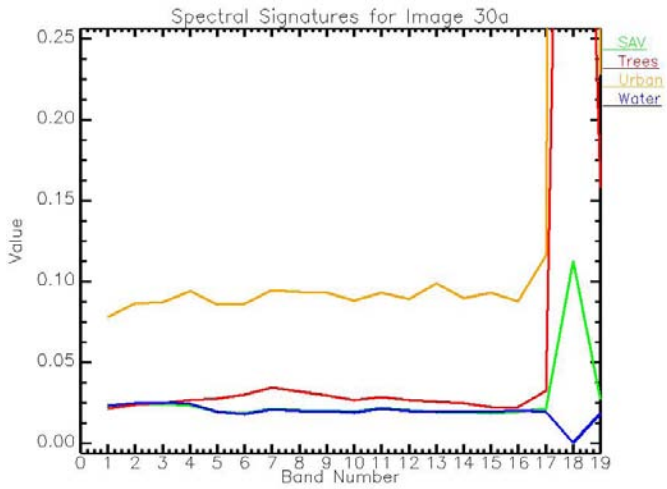

Figure 5a. Spectral signatures of four classes in image 30a

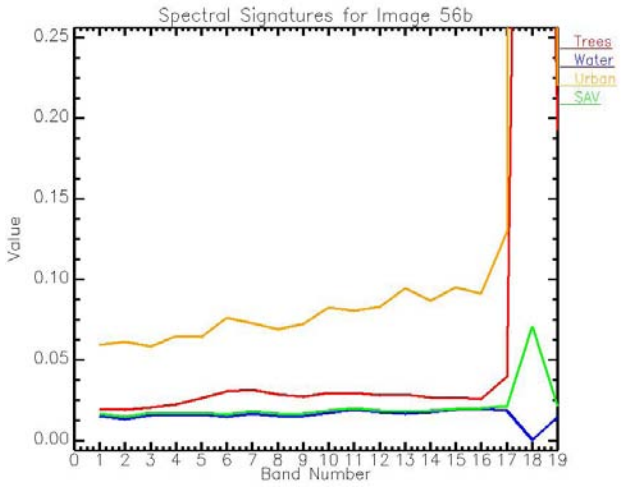

Figure 5b. Spectral signatures of four classes in image 56b

Spectral signatures were also collected in the field with a spectroradiometer (GER1500, Group for Environmental Research, http://www.ger.com/1500.html) in the fall of 2005, to improve the SAM classification scheme and to make suggestions for band placement in the next round of data collection. These ground-based signatures were

imported to a spreadsheet and convolved to match the 19 unique bands of the imagery. Spectral reflectance information was collected for dense eelgrass (*Vallisneria americana*), algal blooms (*Microcystis spp.*), dense waterlily (*Nymphaea spp.*), hydrilla (*Hydrilla verticillata*), periphyton, sand bottom at approximately 20-cm depth, mud bottom at approximately 2-m depth, and open water.

Spectral Library—A spectral library is a collection of reflectance spectra for natural and/or man-made materials for use in identifying unknown spectra. For the images in the pilot study, the signatures collected in the field (22 signatures) were added to the four signatures for each class collected from each of the four images (16 signatures) to create a unique spectral library for the St. Johns River, consisting of 38 signatures for both aquatic and terrestrial features. This spectral library was referenced by ENVI to classify the images using the SAM model.

RESULTS AND DISCUSSION

The accuracy of the hyperspectral imagery classification was assessed by comparing SAV bed width (perpendicular to the shoreline) from classified hyperspectral imagery to bed lengths measured from ground-truthing transects in the river. The spatial accuracy of the imagery was much lower along the edges of the imagery. Therefore, transects located near the edges were not used for the accuracy assessment if nearby ground features (e.g., docks, shoreline) were not in good spatial agreement with the referenced DOQQs. Fifty ground-truthing transects were found to be within the spatially accurate portions of the hyperspectral images and were used for measuring classification accuracy.

Bed lengths for the 50 selected ground-truthing transects from 2003 were compared to the bed lengths estimated from the 2003 hyperspectral imagery at the same locations. Overall, the hyperspectral imagery underestimated bed lengths at the 50 transect sites by 22%. However, among individual transects, there were large differences between estimates based on hyperspectral imagery and field measurements.

SAV areas mapped from the classified hyperspectral imagery show 2,140 acres in the mainstem of the river, from Palatka north to the Fuller Warren Bridge in Jacksonville. This estimate is lower than those generated during other years and from other methods (Dobberfuhl 2002, Dobberfuhl and Trahan 2003). However, if the 22% underestimate is considered, that coverage can be revised up to 2,611 acres. This is still low, but 2003 was a relatively severe drought year, and grass bed recession was common in many areas of the river (Sagan 2005). Another factor influencing this estimate is the method of grass bed

delineation. With traditional photo interpretation, small bare areas within grass beds are not as likely to be identified as in hyperspectral imagery classification. Thus the larger number of bare patches, or "holes," will tend to decrease the aggregate areal coverage estimate. It should be noted, because of these types of issues, using different analytical methods comparisons of areal coverage between years is problematic.

The differences between the estimated and measured data occurred for several reasons. First, there was a large degree of variation in quality from image to image. Because standardized spectral libraries were used to classify each image, SAV may not have been correctly identified in lower-quality images. Second, short grass in deep water defies detection. Deep overlying water attenuates the reflected light energy available to the sensor, and there may not have been sufficient sensor sensitivity under those conditions. Finally, of the 19 bands originally chosen for the imagery, only two demonstrated any usefulness in identifying the presence or absence of SAV.

REFERENCES

Batzer, D.P., and S.A. Wissinger. 1996. Ecology of Insect Communities in Nontidal Wetlands. *Annual Review of Entomology* 41: 75–100.

Burns, J.W., Jr., A.D. Chapman, E. Messer, and J.Konwinski. 1997. *Submerged Aquatic Vegetation of the Lower St. Johns River.* Palatka, Fla.: St. Johns River Water Management District.

Dennison, W.C., R.J. Orth, K.A. Moore, J.C. Stevenson, V. Carter, S. Kollar, P.W. Bergstrom, R.A. Batiuk. 1993. Assessing Water Quality With Submerged Aquatic Vegetation. *BioScience* 43: 86–94.

Dobberfuhl, D.R. 2002. *Distribution of Submerged Aquatic Vegetation in the Lower St. Johns River*: *1998 Atlas.* Professional paper 2002-1. Palatka, Fla.: St. Johns River Water Management District.

Dobberfuhl, D.R. and N. Trahan. 2003. *Distribution of Submerged Aquatic Vegetation in the Lower St. Johns River: 2001 Atlas.* Professional paper 2003-1. Palatka, Fla.: St. Johns River Water Management District.

Heck, K.L., and L.B. Crowder. 1991. Habitat Structure and Predator-Prey Interactions in Vegetated Aquatic Systems. In *Habitat Structure: The Physical Arrangement of Objects in Space,* S.S. Bell, E.D. McCoy, and J. Mushinsky, eds., 281–99. New York: Chapman Hall.

Jordan, F., M. Bartolini, C. Nelson, P.E. Patterson, and H.L. Soulen. 1996. Risk of Predation Affects Habitat Selection By the Pinfish *Lagodon rhomboides* (Linaeus).

Journal of Experimental Marine Biology and Ecology 208: 45–56.

Lombardo, P. 1997. Predation by *Enallagma* Nymphs(Odonata: Zygoptera) Under Different Conditions of Spatial Heterogeneity. *Hydrobiologia* 356: 1–9.

Rozas, L.P., and W.E. Odum. 1988. Occupation of Submerged Aquatic Vegetation By Fishes: Testing the Roles of Food and Refuge. *Oecologia* 77: 101–06.

Sagan, J.J. 2005. *A Reanalysis of Data Related to Submerged Aquatic Vegetation Within the Lower St. Johns River: 1996–2005.* Final report. Palatka, Fla.: St. Johns River Water Management District.

Scheffer, M. 1998. *Ecology of Shallow Lakes*. London: Chapman Hall.

Solimini, A.G., G.A. Tarallo, and G. Carchini. 1997. Life History and Species Composition of the Damselfly Assemblage Along the Urban Tract of a River in Central Italy. *Hydrobiologia* 356: 21–32.